Heliyon 10 (2024) e27140

Contents lists available at ScienceDirect

Heliyon

journal homepage: www.cell.com/heliyon

Research article

Experimental study on the effects of pressure loss on uniformity, application rate and velocity on different working conditions using the dynamic fluidic sprinkler

Xingye Zhu [a], Alexander Fordjour [b], Frank Agyen Dwomoh [b], Joseph Kwame Lewballah [a,c], Samuel Anim Ofosu [b], Junping Liu [a], Xiu Dai [d,*], James Oteng [b]

[a] *Research Centre of Fluid Machinery Engineering and Technology, Jiangsu University, Zhenjiang 212013, China*
[b] *Faculty of Engineering, Koforidua Technical University, Koforidua, Eastern Region, Ghana*
[c] *Faculty of Engineering and Technology, Department of Mechanical Engineering, Kumasi Technical University, Kumasi, Ashanti Region, Ghana*
[d] *Key Laboratory of Smart Agricultural Technology (Yangtze River Delta), Ministry of Agriculture and Rural Affairs, PR China, Nanjing, 210044, China*

A R T I C L E I N F O

Keywords:
Space
Pressure
Nozzle
Uniformity
Droplet
Velocity
Fluidic sprinkler

A B S T R A C T

An experiment was conducted to determine the effects of pressure loss, combined spacing, and. coefficients of uniformity on the dynamic fluidic sprinkler. Spline interpolation was used to convert the radial water volume into grid-type data and various pressure conditions were used to simulate the three-dimensional water distribution under square and triangular combinations of sprinklers. For each of the combinations of the sprinklers, experiments were performed at operating pressures of 0.15, 0.2, 0.25, and 0.3 MPa, respectively. To find the optimum spatial distribution of sprinklers, three different sprinkler intervals, 1R, 1.2R, and 1.4R, were performed for the square and triangular combinations. The droplet size distributions were also measured along a radial transect from the sprinkler for each operational pressure using the Thies Clima Laser Precipitation Monitor. The results demonstrated that the average values of the inclination angles of the water droplet trajectory curves were 60.78° and 68.85° as the pressure rose from 0.15 MPa to 0.3 MPa. When the pressure exceeds 0.2 MPa, the square combination's distribution uniformity coefficients of 25% low and high values were higher than those of the triangle combination. Triangular combination coefficients of uniformity (CU) values initially decreased and then increased as sprinkler spacing increased, with the CU value under 1.4R spacing reaching 73.85%. At a 1.2R interval, the CU value of a triangular combination was 8.49% lower than that of a square combination, which is a significant difference. Peak irrigation values for the square combination, when the pressure was changed from 0.1 to 0.3 MPa, were 29.97, 22.9, 19.8, 19.91, and 19.21 mm h^{-1}, respectively. The CU values at 0.2, 0.25, and 0.3 MPa decreased at rates of 0.07%, 1.36%, and 0.8%, respectively, when the pressure was reduced by 10%.

* Corresponding author.
E-mail addresses: zhuxy@ujs.edu.cn (X. Zhu), fordjouralexander27@yahoo.com (A. Fordjour), frank.agyendwomoh@ktu.edu.gh (F. Agyen Dwomoh), jleo440@gmail.com (J. Kwame Lewballah), ofosu@ktu.edu.gh (S. Anim Ofosu), liujp@ujs.edu.cn (J. Liu), 20170009@jaas.ac.cn (X. Dai), otengk7@gmail.com (J. Oteng).

https://doi.org/10.1016/j.heliyon.2024.e27140
Received 2 November 2023; Received in revised form 20 February 2024; Accepted 25 February 2024
Available online 27 February 2024
2405-8440/

1. Introduction

One of the most used irrigation techniques for agriculture is sprinkler irrigation. Irrigation techniques have been used to increase agricultural output in arid areas and in locations where rainfall is the main factor in crop development. Additionally, irrigation engineering can generate a more feasible timetable and control the amount of irrigation used [1–3]. Sprinkling irrigation systems are used as a part of irrigation system applications all around the world because of how convenient they are to use. Additionally, for a variety of soil types and topographical situations, this type of irrigation delivers the correct combination of water distribution, precision control over irrigation depth, and high applied irrigation efficiency [4–6]. Based on their modes of operation, rotating sprinklers come in a variety of designs, including impeller-type, fluidic, responding force, and impact sprinklers [7,8]. The performance of a sprinkler is influenced by its discharge, wetted radius, distribution pattern, application rate, and droplet sizes, according to Refs. [9,10]. The depth of water applied to the area per unit of time is known as the water application rate. The water application rate has implications on which sprinkler should be used for a specific soil, crop, and operating environment. The operating pressures, nozzle size, and sprinkler spacing all affect the application rate [11,12]. However, compared to the impact of the sprinkler nozzle on the application rate, the impact of operating pressure on application rate is negligible [13–15]. It has been discovered that a sprinkler nozzle that disperses tiny droplets has the highest average application rate and covers the smallest wetted area. Since the sprinkler discharge tends to expand more quickly than the wetted area, increasing the nozzle diameter increases the average application rate [16–18]. [19] reported that the operating pressure, sprinkler size, and sprinkler spacing have the most effects on the application uniformity of a sprinkler, which is a crucial performance parameter for the design and evaluation of sprinklers. According to Refs. [20,21], a coefficient of uniformity (CU) value of 85% or higher is “desirable,” while one less than 85% is deemed to be “low”. Christiansen’s coefficient of uniformity is the parameter that is most frequently used to evaluate the uniformity of the water distribution in sprinkler irrigation, [22,23]. According to Refs. [24,25], irrigation water kinetic energy and wind drift are directly impacted by drop size distributions. In the study [26,27], the droplet size characteristics of a full fluidic sprinkler were investigated. It was found that 50% of the droplets had a diameter of less than 0.5 mm and that at most distances, droplets with a diameter of less than 2 mm made up 50% of the water volume.

A lot of work has been done on the dynamic fluidic sprinkler mostly under indoor and quite a few outdoor conditions. However, these research works have not extensively addressed sprinkler spacing and pressure loss. Therefore, the objective of this study was to examine the effects of pressure variation on the combined spacing of sprinklers, application uniformity, application rate and velocity in different working conditions.

2. Materials and Methodology

The study was performed in the indoor sprinkler irrigation laboratory at Jiangsu University. The sprinkler spraying test system is mainly composed of a centrifugal pump, electromagnetic flowmeter, pressure gauge, flow control valve, pressure regulator, return valve, water delivery pipe, sprinkler and other devices. The schematic diagram is shown in Figs. 1 and 2 shows the test site map.

The sprinkler head was positioned at a 90-degree angle to the ground on a 1.4-m riser. Catch cans with dimensions of 200 mm in diameter and 600 mm in height were utilized for the experiment. Before the experiment, the sprinkler was run for a few minutes to standardize the environment. The operating pressure at the base of the sprinkle head was regulated and maintained by a valve with the aid of a pressure gauge with an accuracy of ±1%. Operating pressures that corresponded to each value were 0.15, 0.2, 0.25, and 0.3 MPa. Measurements of the depth of the water were applied in line with [28]. The experiment lasted for an hour, and a graduated measuring cylinder was used to determine the water depth in the catch cans. The distribution of sprinkler water volume at various combination intervals was obtained by linearly superposing the water volume of a single sprinkler at a mounting height of 1.4 m. Square and triangular combinations of the sprinklers, as shown in Fig. 2, were performed for the superposition of the water distribution for each operating pressure. The multiple sprinkler irrigation with the square combination was arranged such that sprinklers were placed in each of the four quadrants of the single sprinkler spraying area at one of the square’s four vertices. The water distribution in the superposition domain was symmetrical. To find the optimum spatial combination of sprinklers, for each of the two combinations of the sprinklers, experiments were performed at the specified operating pressures respectively, at three different sprinkler intervals,

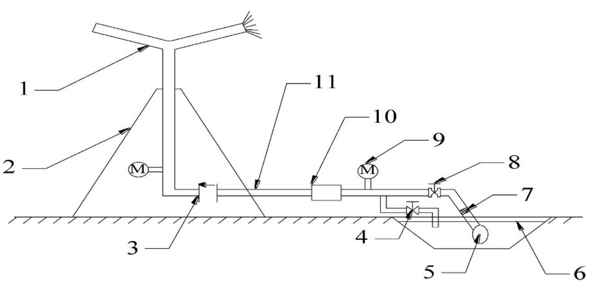

Fig. 1. Schematic view of the indoor sprinkler system
1. Nozzle 2. Fixed bracket 3. Pressure regulator 4. Return valve 5. Water pump 6. Reservoir 7. Filter 8. Flow control valve 9. Pressure gauge 10. Electromagnetic flowmeter 11. Water delivery pipe.

namely 1R, 1.2R, and 1.4R. Where R is the radius of throw of the sprinkler at the specified operating pressure. The droplet size distributions were also measured at intervals of 2 m along a radial transect from the sprinkler for each operational pressure. To guarantee that a significant number of drops travelled through the measured area for each droplet measurement, the sprinkler was allowed to rotate over the Thies Clima Laser Precipitation Monitor (TCLPM) at least five times. A minimum of three replication evaluations were performed for each pressure, and the average value was calculated.

2.1. *Christiansen's coefficient of uniformity* (CU)

The most popular and widely acknowledged uniformity criterion is Christiansen's coefficient of uniformity [38]. Therefore, the coefficient of uniformity (%) was calculated using Christiansen's equation.

$$CU = \Big(\tag{1}$$

$$h^{--} = \frac{\sum_{i=1}^{n} h_i}{n} \tag{2}$$

$$\Delta h = \frac{\sum_{i=1}^{n} |h_i - h|}{n} \tag{3}$$

In the formula, CU indicates coefficient of uniformity; h^{--} represents the average spraying water depth (mm) on the sprinkling irrigation area; Δh deviation of observation from the mean; h_i represents the average dispersion of spraying water depth at each measuring point (mm) and n represents the total number of measuring points.

2.2. *Distribution **uniformity** coefficient (DU)*

The distribution uniformity coefficient refers to the ratio of the average value of the water depth of some measuring points to the average value of the total water depth, which can be divided into 1/4 low-value distribution uniformity coefficient DU_{lq}, 1/4 high-value distribution uniformity coefficient DU_{hq}, and 1/2 low-value distribution Uniform coefficient DU_{lh} and 1/2 high-value distribution uniform coefficient DU_{hh} [29–31]. The distribution uniformity coefficient of sprinkler irrigation emphasizes the hazards caused by local insufficient or excessive irrigation, and the calculation formula is as follows:

$$DU_{lq} = \frac{4\sum_{i=1}^{\frac{n}{4}} h_i}{\sum_{i=1}^{n} h_i} \times 100\% \tag{4}$$

$$DU_{hq} = \frac{4\sum_{\frac{3n}{4}}^{n} h_i}{\sum_{i=1}^{n} h_i} \times 100\% \tag{5}$$

$$DU_{lh} = 2\frac{\sum_{i=1}^{\frac{n}{2}} h_i}{\sum_{i=1}^{n} h_i} \times 100\% \tag{6}$$

$$DU_{hh} = \frac{2\sum_{\frac{n}{2}}^{n} h_i}{\sum_{i=1}^{n} h_i} \times 100\% \tag{7}$$

Fig. 2. Schematic view of the experimental setup.

Where DU_{lq} and DU_{hq} are water distribution uniformity coefficients in respect to the 25% lowest and highest parts of the data; n is a quarter of the total number catch can, and h_{ilq} and h_{ihq} are the collected irrigation depth that represents the highest part and lowest part, respectively, DU_{lh}, DU_{hh} is 50% low and the high water distribution uniformity coefficient, and n is half of the total number of the catch can.

To describe the stability of the above-mentioned hydraulic performance when the sprinkler is working, the standard deviation (*STD*) and the variation coefficient (*CV*) are used to analyze the data, and the calculation formulas are (8) and (9) [32,40].

$$STD = \sqrt{\frac{1}{n-1}\sum_{i=1}^{n}\Big(} \tag{8}$$

$$CV = 100 \times \frac{STD}{h^{--}} (\%) \tag{9}$$

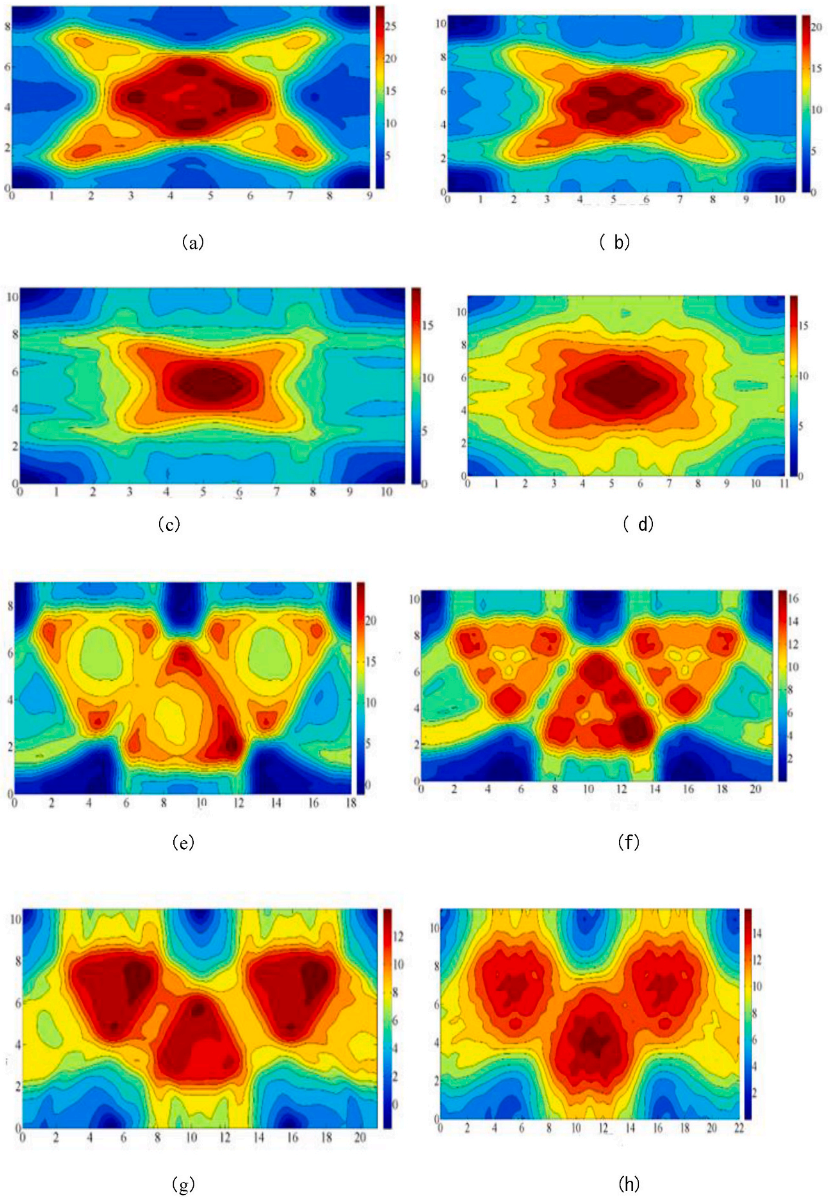

Fig. 3. (a–h).Water distribution of combined sprinkler at different pressures.
Note: (a), (b), (c) and (d) are square combinations with pressures of 0.15, 0.20, 0.25 and 0.3 MPa, respectively. (e), (f), (g) and (h) are triangular combinations of pressure 0.15, 0.20, 0.25 and 0.3 MPa, respectively.

Where h_i represents the *i*-th water depth value (mm) of each measuring point arranged from small to large; n represents the total number of measuring points and h^{--} represents the average spraying water depth (mm) on the sprinkling irrigation area.

3. Results and Discussion

3.1. Water distribution of combined sprinklers

Fig. 3 shows the combined sprinkler water distribution at various pressures of 0.15, 0.2, 0.25 and 0.3 MPa. From Fig. 3 (a)–(d), it is evident that the irrigation volume of the square combination of sprinklers is primarily concentrated in its center and gradually declines along its four vertices. The triangular combination of sprinklers in Fig. 3 (e)–(h) shows that there are three visible water concentration locations. Table 1 shows the water volume distribution for CU, DU_{lq}, DU_{hq}, DU_{lh}, and DU_{hh} at various pressures. Peak irrigation values for the square sprinkler configuration were 29.97, 22.9, 19.8-, and 19.21-mm h-1 when the pressure was reduced from 0.15 to 0.3 MPa. When the pressure was increased by 50% at 0.15 MPa, the peak irrigation value dropped by 23.59%. The highest irrigation value dropped by 3.61% when the pressure was increased by 200%. It demonstrates how irrigation peaks tend to stabilize as pressure rises, this conclusion is similar to previous results obtained by Refs. [32–34]. The triangle combination's highest values were 26.39, 17.84, 14.99-, and 16.9 mm h^{-1}, in that order. The triangle combination's peak values first decreased and then increased as pressure increases from 0.15 to 0.3 MPa. For the square combined sprinklers, the distribution uniformity coefficients and CU values had the following relationship: $DU_{hq} > DU_{hh} > 1 > DU_{lh} > CU > DU_{lq}$. This shows how the sprinkler intensity of square combinations connected in the sequence of largest value to least value increases in high-pressure circumstances. The average value of these two locations tends to be the average sprinkler intensity in the high-value and low-value areas of the same area. The relationship between the distribution uniformity coefficient and the CU value of a triangular combination sprinkler irrigation is $DU_{hq} > DU_{hh} > 1 > DU_{lh} > CU > DU_{lq}$ when the operating pressure was varied from 0.15 to 0.20 MPa. It demonstrates that the sprinkler effect is widespread and that the triangular combined sprinkler intensity changes quickly between the maximum and minimum values under 0.15–0.20 MPa. The link between the distribution uniformity coefficient and the CU value is $DU_{hq} > DU_{hh} > 1 > CU > DU_{lh} > DU_{lq}$, and the sprinkler watering impact is better when the pressure rises over 0.25 MPa (see Fig. 4).

Table 1 shows the combined coefficient of uniformity under different pressures. It can be seen from Table 1 that when the pressure exceeds 0.2 MPa, the square combination's DU_{lq} and DU_{lh} values are higher than those of the triangle combination, while the square combination's DU_{hq} and DU_{hh} values are lower. The square combination's DU_{lq} and DU_{lh} values increased as the working pressure increased, but its DU_{hq} and DU_{hh} values were reduced. It demonstrates that, as pressure increases, the portion of low-value areas in the total sprinkler intensity in the square combined sprinkler irrigation rises while the portion in the high-value area declines. Therefore, increasing the operating pressure for the dynamic fluidic sprinkler under the square combination will help to improve the uniformity in the spraying area. However, increasing operating pressure to improve upon the uniformity will impact negatively the energy-saving potential of the dynamic fluidic sprinkler. There is therefore the need for further optimization to improve the uniformity under low operating pressure conditions to ensure the energy-saving potential of the sprinkler.

The actual sprinkler irrigation system experiences some pressure loss as a result of the influence of numerous factors. The effect of lowering operating pressure on the uniformity of combined spraying was examined using a square configuration. Table 2 shows the relationships between the CU value and the distribution uniformity coefficient under the working conditions. In general, for both square and triangular combinations, the CU values decreased linearly with decreasing pressure. Specifically, the CU values for the square combination decreased linearly from 78.97% to 55.93% with decreasing pressure from 0.3 MPa to 0.15 MPa. Similarly, the

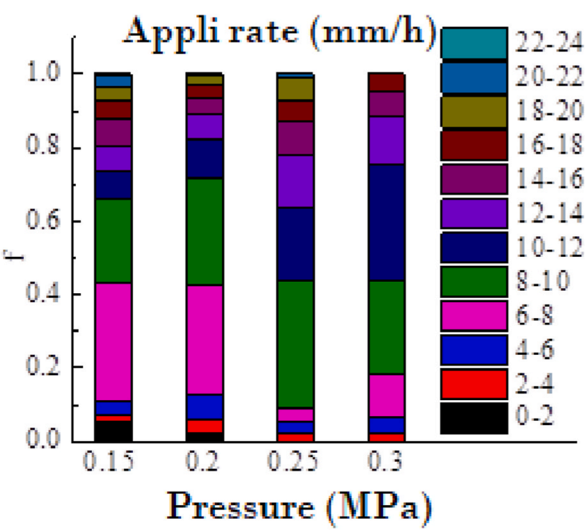

Fig. 4. Column distribution of applications rate [39].

Table 1
Combined uniformity coefficient under different pressures.

Pressure (MPa)	Combination	Application rate (mm h^{-1})	CU/%	DU_{lq}/%	DU_{hq}/%	DU_{lh}/%	DU_{hh}/%
0.15	square	29.97	55.93	45.28	172.03	57.00	143.00
	triangle	26.39	64.31	41.25	149.86	66.68	133.32
0.20	square	22.90	62.39	51.47	168.38	66.50	133.50
	triangle	17.84	64.02	38.46	153.43	65.15	134.85
0.25	square	19.80	71.74	58.57	150.37	73.67	126.33
	triangle	14.99	67.24	45.27	153.46	65.24	134.76
0.30	square	19.21	78.97	66.76	135.14	75.20	124.80
	triangle	16.90	74.20	55.89	137.63	72.36	127.64

Table 2
Combined uniformity coefficients under pressure loss.

	pressure (MPa)	pressure reduction /MPa	CU%	DU_{lq}%	DU_{hq}%	DU_{lh}%	DU_{hh}%
1	0.15	0.135	64.25	51.22	168.63	67.04	132.96
2	0.2	0.18	71.69	56.95	155.02	71.81	128.19
3	0.25	0.225	74.49	65.9	145.55	75.3	124.7
4	0.3	0.27	78.34	64.51	137.48	78.55	121.45

triangular combination decreased linearly from 74.2% to 64.31% within the same operating pressure range. The above finding demonstrates that pressure reduction does not always result in lower uniformity of sprinkler irrigation.

The peak values of the application rate for operating pressures of 0.15, 0.2, 0.25 and 0.3 MPa are 22.05, 20.07, 20.16- and 17.92-mm h^{-1}, respectively. The absolute value of the peak change amplitude of the sprinkler application rate is less than 7%, indicating again that within the operating pressure range, reducing the pressure by 10% had little impact on sprinkler application uniformity.

3.2. Distribution characteristics of water droplet velocity

The frequency distribution of droplet velocity at various operating pressures is depicted in Fig. 5. Fig. 5(a) shows that, under pressures of 0.15 MPa and 0.2–0.3 MPa, the horizontal velocity of water droplets essentially coincides and deviates greatly from the frequency curve, suggesting that the pressure had little impact on the distribution of the horizontal velocity of sprayed water droplets. This confirmed the condition in Table 3 that the nozzle's range tends to increase gradually after 0.2 MPa of pressure. The number of

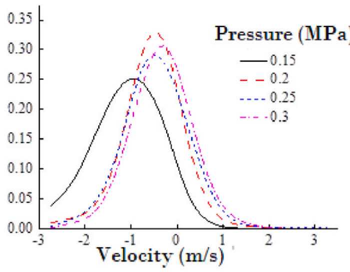

（a） Horizontal direction

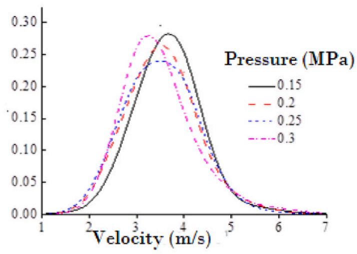

（b） Vertical direction

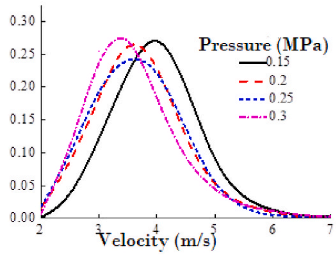

（c） Average speed

Fig. 5. (a–c). Frequency distribution of droplet velocity.

water drops travelling to the right increases as the frequency of water drops in the 0–0.25 m/s range steadily increases with pressure, demonstrating that the pressure increase intensifies the collision between water drops. It can be seen from Fig. 5 (b) that the velocity of water droplets in the vertical direction decreases with the increase of pressure, which is consistent with the rule that the range of the nozzle increases with the increase of pressure. The velocity in the vertical direction does not appear as negative as it does in the horizontal direction, indicating that the velocity direction in the vertical direction will not change due to the impact of gravity, although the water droplets will collide during movement. Fig. 5 (c) shows that the frequency curve moves to the left with the increase of pressure, indicating that the resultant velocity of the water droplet group at the same location decreases with the increase of pressure.

Table 3 demonstrates the maximum, minimum and average values of water droplet velocity at a distance of 6,7 and 8 m. It can be seen from Table 3 that the distribution range of water droplet velocity at a distance of 8 m at a pressure of 0.3 MPa is wide, ranging from 2.93 ms-^{1} to 12.53 m s-^{1}, with a fluctuation amplitude of 9.6 ms-^{1}. When the pressure was 0.3 MPa, the water droplet velocity distribution at 8 m away from the nozzle had great variability, and its variability is 18.84%, which is 119% higher than that at 0.2 MPa and 7 m away from the nozzle. The trajectory curve of water droplets sprayed by the nozzle moving in the air for 53ms-^{1} at a distance of 9 m away from the nozzle is shown in Fig. 6.

It is demonstrated in Fig. 6 (a) that the main distribution ranges of water dropping velocity, horizontal velocity and vertical velocity are 3~5.5 m/s, 3~1 m/s and 2.5–5.5 m/s, respectively at distances of 5 m and 0.2 MPa from the nozzle.

Fig. 7 shows the frequency distribution curve of water droplet velocity at 6, 7 and 8 m away from the nozzle under 0.2 MPa pressure. It can be seen from Fig. 7 (a) that at the distance of 6~8 m from the nozzle, the distribution range of water droplet velocity is respectively - 4.5~2 m/s, - 7.25–1.25 m/s and - 8.75–0.25 m/s, which indicates that with the increase of distance, the number of high-speed water droplets increased and the number of low-speed water droplets decreased. From Fig. 7. (b), it can be observed that at 6~8 m, the vertical velocity curve of water droplets is almost parallel at the rising stage and the falling stage, and the frequency of water droplets at 4.25–4.5 m/s, 4.75~5 m/s and 5.25–5.5 m/s are 37.84%, 33.9% and 30.8%, respectively. The vertical component of the velocity of very few water drops is as high as 10 m/s. It can be seen from Fig. 7 (c) that the resultant velocity of water drops is below 12 m/s, which indicates that the vertical component of the velocity of this part of water drops is quite different from the horizontal component, and the vertical component is dominant, and the water drops fall rapidly not far away. Compared with the frequency curve of water droplet velocity at 6 m and 7 m away from the nozzle, the curve at 8 m is narrower and the distribution of water droplet velocity is more concentrated.

Fig. 8 presents the inclination angle of the water droplet trajectory curve at various pressures. The distribution range of the inclination angle of the water droplet trajectory curve as the pressure was varied from 0.2 to 0.3 MPa was found to be 54 to 64, 59 to 71, and 59–79°, respectively. The distribution curves are fitted using a logarithmic normal, with fitting degrees R^2 values of 0.95, 0.88, and 0.84, mean values of 58.77, 65.77, and 69.25, and standard deviations of 0.025, 0.035, and 0.049. The average values of the inclination angles of the water droplet trajectory curves ranged from 60.78° to 68.85°, respectively, increasing by 13% as the pressure increased from 0.2 MPa to 0.3 MPa. It demonstrates that for the dynamic fluidic sprinkler, as pressure increases, the greater the angle of inclination of the water droplet movement track at the same measuring point, the greater the likelihood of damage to crops caused by water droplets with the same kinetic energy intensity, and the more likely it is to cause soil hardening and damage the soil structure.

From the above analysis, of the coefficient of uniformity, application rate and velocity it was found that 0.20 MPa performed best. A further test was carried out with 0.20 MPa to find the spatial distribution for combination of the sprinklers with 1R, 1.2R, and 1.4R as sprinkler spacing. The core irrigation peak region gradually reduces as the combined spacing rises and a water volume peak emerges in the surrounding direction. The triangular combination contains three peak areas that resemble the triangle when the total sprinkler spacing is 1R. The triangle's area steadily reduces as the combined spacing increases and the peak water volume emerges in the direction of the triangle's center vertical line. The findings are provided in Table 4. With an increase in combination spacing, the peak irrigation values in the square and triangular combined sprinkler irrigation areas decreased. The highest irrigation values in the two combinations were 10.54 and 10.26 mm h^{-1} at 1.4R spacing, respectively, which were 47% and 32% reduction from 1R spacing. Under 1R–1.4R combined spacing, the square combination's irrigation peak value was higher than that of the triangle combination,

Table 3
Statistical characteristics of water drop velocity.

Pressure (MPa)	Distance from nozzle (m)	Minimum ($m \cdot s^{-1}$)	Maximum ($m \cdot s^{-1}$)	Variation (%)
1.5	6	1.75	6.98	10.48
	7	2.94	10.69	15.5
	8	3.68	8.97	9.29
0.2	6	1.76	7.97	15.28
	7	3.88	11.62	8.6
	8	4.07	9.76	11.2
0.25	6	2.18	7.99	17.75
	7	2.33	9.14	15.54
	8	3.02	10.77	16.58
0.3	6	0.43	1.51	18
	7	2.32	8.17	15.8
	8	2.93	12.53	18.84

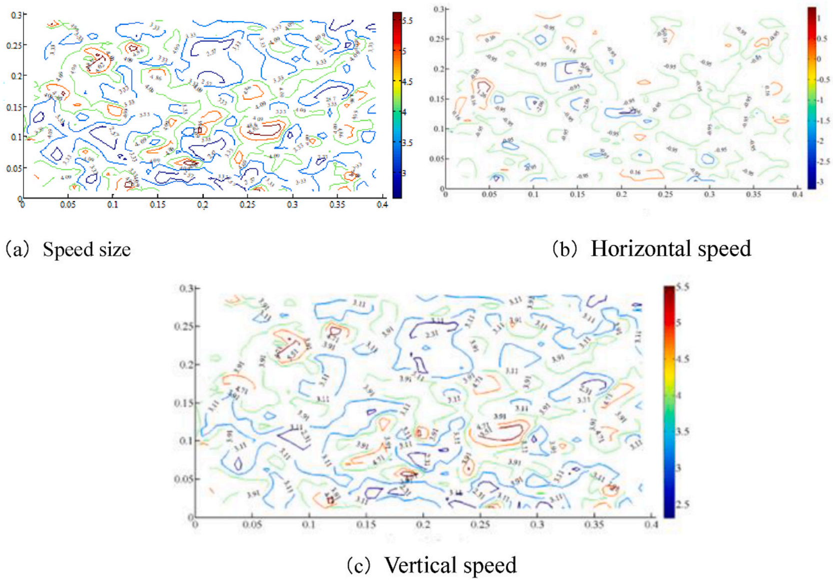

Fig. 6. (a–c). Cloud map of droplet velocity distribution [2].

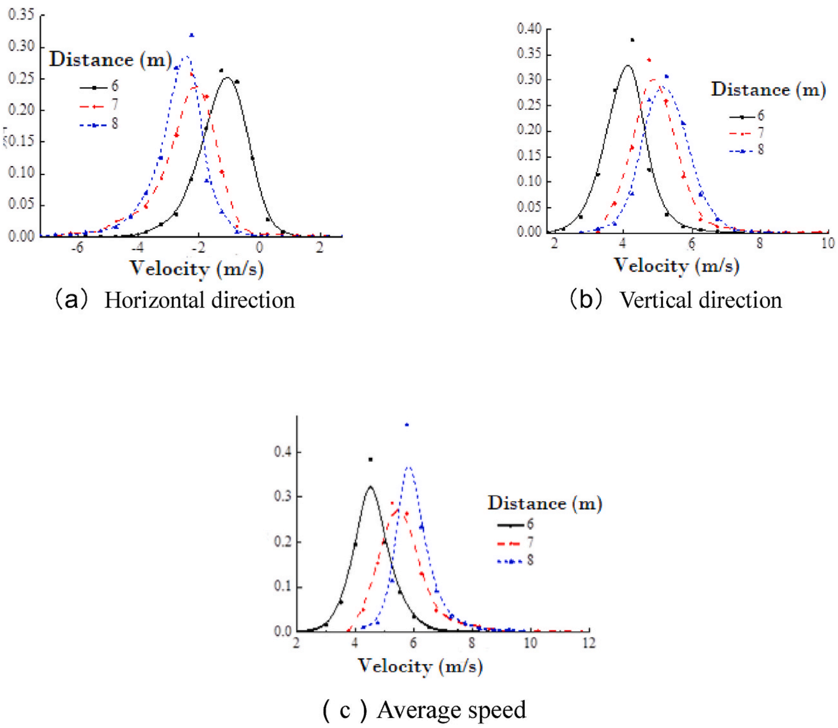

Fig. 7. (a-c).Velocity distribution at 0.2 MPa pressure.

with a difference of 4.76 mm h^{-1}, The square combined irrigation peak value at 1R combined spacing was higher than all other combined forms in Fig. 9, with a value of 19.91 mm h^{-1}, which means that in the actual sprinkler irrigation system, the sprinkler should not operate too close to this working condition to prevent water and soil loss.

The relationship between the distribution uniformity coefficient and the CU value for the square and triangle combination at 1.2R and 1.4R spacing is shown in Table 4. It demonstrates that, in the case of combined sprinkling irrigation, the sprinkling intensity is typically related from the greatest value to the lowest value. There is a noticeable difference between the average value and the average sprinkling intensity in the same area's high-value area and low-value area, but the sprinkling effect is widespread. Under the

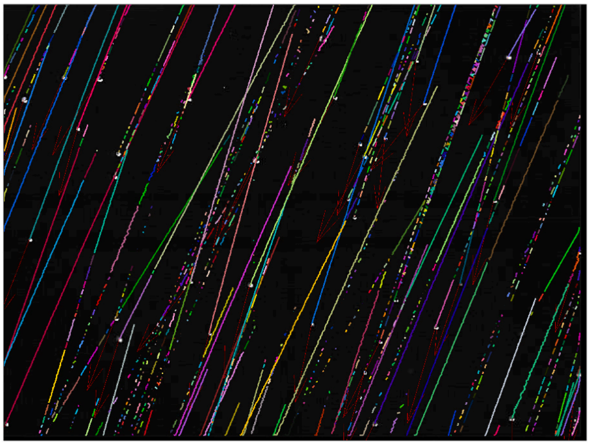

Fig. 8. Water droplet trajectory at 9 m from the nozzle.

Table 4
Combined uniformity coefficients at different combinations of spacing.

Pressure (MPa)	Combination form	Combined spacing	Peak irrigation/mm h^{-1}	CU/%	DU_{lq}/%	DU_{hq}/%	DU_{lh}/%	DU_{hh}/%
0.20	square	1R	19.91	75.52	65.22	138.98	73.28	126.72
	triangle	1R	15.15	72.21	54.44	136.48	71.21	128.79
	square	1.2R	15.34	74.11	54.43	133.57	75.44	124.56
	triangle	1.2R	14.95	65.62	53.59	151.81	66.66	133.34
	square	1.4R	10.54	70.18	64.48	152.9	72.55	127.45
	triangle	1.4R	10.26	73.85	70.37	148.55	76.9	123.1

combination of a square and a triangle with a 1R spacing, the relationship between the CU value and the distribution uniformity coefficient is $DU_{hq} > DU_{hh} > 1 > CU > DU_{lh} > DU_{lq}$. It was found that the sprinkler application rate is more effectively connected in the sequence of highest to lowest value under this combined sprinkler irrigation condition. The difference between the average value and the average sprinkler application rate is close in the same area's high-value area and low-value area, and the sprinkler irrigation effect is better. The DU_{lq} and DU_{lh} values of the square combination are bigger than those of the triangle combination at the combined spacing of 1R and 1.2R, while their DU_{hq} and DU_{hh} values are lower than those of the triangle combination. It was demonstrated that the proportion of square combination sprinkling intensity in the total application rate in the low-value area is higher than that in the triangle combination; the proportion of square combination sprinkling intensity in the total application rate in the high-value area is lower than that of triangular combination; and the combined spacing of 1.4R is the opposite of the above. The CU value of square combined sprinklers drop as sprinkler spacing increases; however, the CU value is still greater than 70% when the combined sprinkler spacing ranges from 1R to 1.4R. As sprinkler distance increased, the triangular combination sprinkler's CU value first decreased and then increased, reaching 73.85% under 1.4R spacing. These results are slightly better than those obtained by previous researchers for the complete fluidic sprinkler [35–37]. The triangle combination's CU value at the 1.2R interval is 8.49% lower than the square combination's, which is a significant difference. The triangular combination of 1.4R spacing should be used under the pressure of 0.2 MPa at the installation height of 1.4 m.

4. Conclusions

The evaluation indexes used include water application, coefficient of uniformity and Velocity distribution. The following conclusions can be drawn.

- The square combination's 25% low and high values for distribution uniformity coefficients were higher than those of the triangle combination when the pressure was over 0.2 MPa. As sprinkler spacing increased, the triangular combination coefficients of uniformity (CU) value initially declined and then increased, with the CU value under 1.4R spacing reaching 73.85%.
- At a 1.2R interval, the CU value of a triangular combination was 8.49% lower than a square combination, which is a significant difference. Peak irrigation values for the square combination, when the pressure was changed from 0.1 to 0.3 MPa, were 29.97, 22.9, 19.8, 19.91, and 19.21mmh-1, respectively.
- When the pressure was increased by 50% under 0.1 MPa, the peak irrigation value fell by 23.59%. The peak irrigation value was reduced by 33.93% when the pressure was increased by 200%. Most of the irrigation volume produced by the square combination's sprinklers is focused in its center, while the volume of water flowing via its four vertices gradually declines.

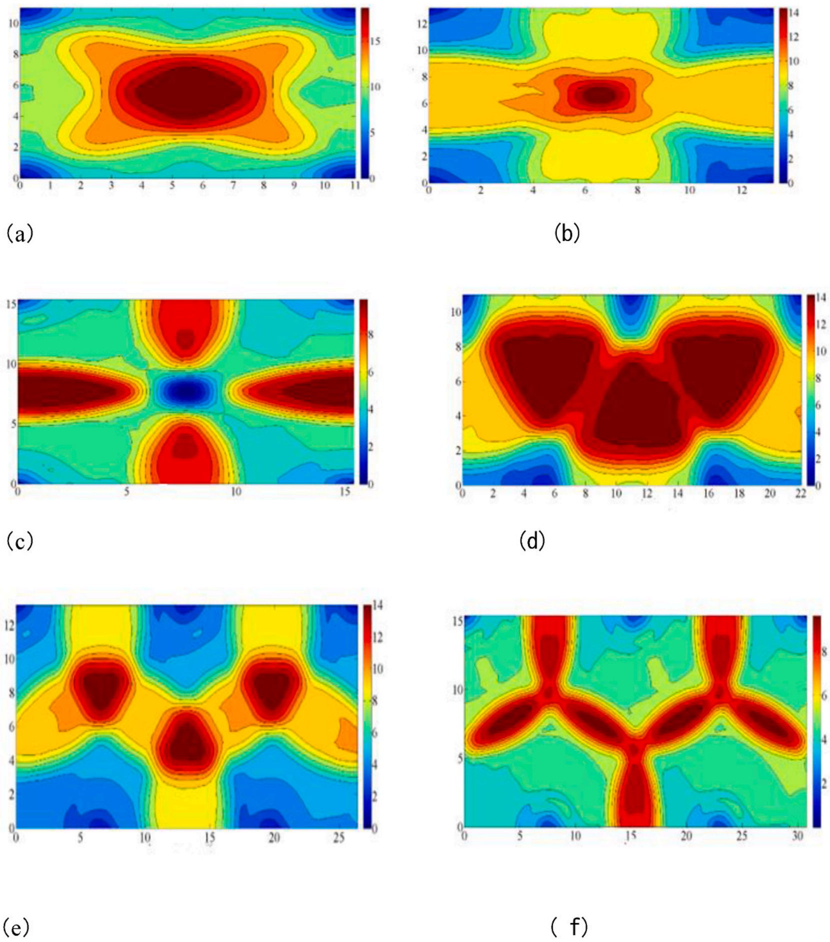

Fig. 9. (a–f). Spatial distribution of combined sprinklers with 1R , 1.2R and 1.4R [24].
Note: (a), (b), and (c) are square combinations with nozzle spacing of 1R, 1.2R, and 1.4R respectively
(d), (e) and (f) are the triangular combination of nozzles with a spacing of 1R, 1.2R and 1.4R respectively.

- ➢ The number of water drops increased as the frequency of water drops in the range of 0–0.25 m/s, indicating that the pressure increase intensifies the collision between water drops.
- ➢ The average values of the inclination angles of the water droplet trajectory curves were 60.78° and 68.85° as the pressure rose from 0.2 MPa to 0.3 MPa.
- ➢ In conclusion, in areas with limited water supply, such as dry and semi-arid regions, it can enhance intensive farming, high-value crop output and quality, and water usage efficiency.

Availability of data and materials

The authors declare that datasets used in the manuscript are readily available upon request from the corresponding author.

CRediT authorship contribution statement

Xingye Zhu: Software, Resources, Conceptualization, Ajani Ibrahm, Funding acquisition, Formal analysis, Data curation, Conceptualization. **Alexander Fordjour:** Writing – review & editing. **Frank Agyen Dwomoh:** Conceptualization. **Joseph Kwame Lewballah:** Writing, review and editing. **Xiu Dai:** Conceptualizatio and methodology. **Samuel Anim Ofosu:** Methodology. **Junping Liu:** Obeng Peprah, Writing – review & editing, Supervision, Resources, Writing – original draft. **James Oteng:** Resources.

Declaration of competing interest

The authors declare the following financial interests/personal relationships which may be considered as potential competing interests: Xingye Zhu reports financial support was provided by: Key Laboratory of Smart Agricultural Technology (Yangtze River Delta),

Ministry of Agriculture and Rural Affairs, P.R.China, Nanjing. Xingye Zhu reports a relationship with: Key Laboratory of Smart Agricultural Technology (Yangtze River Delta), Ministry of Agriculture and Rural Affairs, P.R.China, Nanjing: employment. Xingye Zhu has no patent pending. I have nothing to declare.

Acknowledgements

The authors are greatly indebted to the National Natural Science Foundation of China (No. 52279036), the Key R&D Project of Jiangsu Province (Modern Agriculture) (No. BE2022351), the Project of Faculty of Agricultural Equipment of Jiangsu University (No. NZXB20210101, and the Project of Key Laboratory of Smart Agricultural Technology (Yangtze River Delta), Ministry of Agriculture and Rural Affairs (No. KSAT-YRD2023006) .

References

[1] R.A. Kohl, K.S. Koh, D.W. Deboer, Chemigation drift and volatilization potential, Appl. Eng. Agric. 3 (1987) 174–177.
[2] Z. H Zhang, X. D Sun, J.P. Xie, H. Li, D. J Zhang, T. T Jiang, M. L Lyu, L. Hua, Numerical simulation of water-sand phase flow in regulator channel of micro-sprinkler irrigation system, Journal of Drainage and Irrigation Machinery Engineering 40 (2) (2022) 211–216.
[3] R. Chen, H. Li, Wang, J.X. Guo, Effects of pressure and nozzle size on the spray characteristics of low-pressure, Rotating Sprinklers. Water. 12 (2020) 2904.
[4] X. Jiang, S. Wang, J.J. Chen, C. Zhu, X. Zhu, Analysis of influencing factors on atomization characteristics of fan nozzle, Journal of Drainage and Irrigation Machinery Engineering 40 (10) (2022) 1065–1071.
[5] R.A. Kohl, R.D. Bernuth, G. Heubner, Drop size distribution measurement problems using a laser unit, Trans. ASAE (Am. Soc. Agric. Eng.) 28 (1985) 190–192.
[6] Y. Fukui, K. Nakanishi, S. Okamura, Computer elevation of sprinkler uniformity, Irrigat. Sci. 2 (1980) 23–32.
[7] M. Ge, P. Wu, D. Zhu, L. Zhang, Comparisons of spray characteristics between vertical impact and turbine drive sprinklers—a case study of the 50PYC and HY50 big gun-type sprinklers, Agric. Water Manag. 228 (2020) 105847.
[8] J. Huang, J. Wang, X. Zhao, P. Wu, Z. Qi, H. Li, Effects of permanent ground cover on soil moisture in jujube orchards under sloping ground: a simulation study, Agric. Water Manag. 138 (2014) 68–77.
[9] R.O. Darko, S.Q. Yuan, J.P. Liu, H.F. Yan, X.Y. Zhu, Overview of advances in improving uniformity and water use efficiency of sprinkler irrigation, Int. J. Agric. Biol. Eng. 10 (2017) 1–15.
[10] H.M. Al-Ghobari, Effect of maintenance on the performance of sprinkler irrigation systems and irrigation water conservation, Food Sci. Agric. Res. Cent. Res. Bull. 141 (2006) 1–6.
[11] D.W. DeBoer, M.J. Monnens, D.C. Kincaid, Measurement of sprinkler drop size, Appl. Eng. Agric. 17 (2001) 11–15.
[12] J. Keller, R.D. Bliesner, Sprinkle and Trickle Irrigation, Van Nostrand Reinhold Pun, New York, NY, USA, 1990.
[13] R.A. Kohl, Drop size distribution from medium-sized agricultural sprinklers, Trans. ASAE (Am. Soc. Agric. Eng.) 17 (1974) 690–693.
[14] B.A. King, Moving spray-plate center-pivot sprinkler rating index for assessing runoff potential, Trans. ASABE (Am. Soc. Agric. Biol. Eng.) 59 (2016) 225–237.
[15] Z. Zhu, D. Zhu, M. Ge, The spatial variation mechanism of size, velocity, and the landing angle of throughfall droplets under maize canopy, Water 13 (2021) 2083.
[16] J.P. Liu, X.Y. Zhu, S.Q. Yuan, J.H. Wan, P. Chikangaise, Hydraulic performance assessment of sprinkler irrigation with rotating spray plate sprinklers in indoor experiments, J. Irrig. Drain Eng. (2018) 144.
[17] J. Li, M. Rao, Sprinkler water distributions as affected by winter wheat canopy, Irrigat. Sci. 20 (2000) 29–35.
[18] N. Zapata, O. Robles, E. Playán, P. Paniagua, C. Romano, R. Salvador, F. Montoya, Low-pressure sprinkler irrigation in maize: differences in water distribution above and below the crop canopy, Agric. Water Manag. 203 (2018) 353–365.
[19] J. Liu, J. Xu, T. Li, M. Zaman, Relationship between solar energy and sprinkler hydraulic performance of solar sprinkler irrigation system, Journal of Drainage and Irrigation Machinery Engineering 39 (6) (2021) 637–642.
[20] L. Zhang, X. Hui, J. Chen, Effect of terrain slope on water distribution and application uniformity for sprinkler irrigation, Int. J. Agric. Biol. Eng. 11 (2018) 120–125.
[21] J. Montero, J.M. Tarjuelo, Sprinkler droplet size distribution measured with an optical spectropluviometer, Irrigat. Sci. 22 (2003) 47–56.
[22] O. Robles, E. Playán, J. Cavero, N. Zapata, Assessing low-pressure solid-set sprinkler irrigation in maize, Agric. Water Manag. 191 (2017) 37–49.
[23] L. Zhang, G.P. Merkley, P. Wu, D. Zhu, Effect of catch-can spacing on calculation of sprinkler irrigation application uniformity, CLEAN Soil Air Water 46 (2018) 1800130.
[24] X. W Wang, S.Q. Yuan, W. D Jia, Current situation and development of agricultural mechanization in hilly and mountainous areas, Journal of Drainage and Irrigation Machinery Engineering 40 (5) (2022) 535–540.
[25] R. Salvador, C. Bautista-Capetillo, J.Zapata Burguete, N.A. Serreta, E. Playán, A photographic method for drop characterization in agricultural sprinklers, Irrigat. Sci. 27 (2009) 307–317.
[26] A. Thompson, J.R. Gilley, J.M. Norman, Sprinkler water droplet evaporation a plant canopy model, Trans. ASARE. 36 (1993) 743–750.
[27] L. Tang, S. Yuan, J. Liu, Z. Qiu, J. Ma, X. Sun, C. Zhou, Z. Gao, Challenges and opportunities for development of sprinkler irrigation machine in China, Journal of Drainage and Irrigation Machinery Engineering 40 (10) (2022) 1072–1080.
[28] American Society of Biological Engineers, Procedure for Sprinkler Testing and Performance Reporting, American Society of Biological Engineers, St. Joseph, MI, USA, 1985. ASAE S398.1.
[29] Z. Xu, H. Li, Q.W.J. Xiang, Y. Jiang, J. Liu, Effect on combination irrigation of low pressure 20PY2 impact sprinkler with and without aeration, Journal of Drainage and Irrigation Machinery Engineering 40 (1) (2022) 74–79.
[30] Y. Xu, J. Ge, S. Tian, S. Li, A.L. Nguy-Robertson, M. Zhan, C. Cao, Effects of water-saving irrigation practices and drought resistant rice variety on greenhouse gas emissions from a no-till paddy in the central lowlands of China, Sci. Total Environ. 505 (2015) 1043–1052.
[31] L. Yu, N. Li, X. Liu, Q. Yang, J. Long, Influence of flushing pressure, flushing frequency and flushing time on the service life of a labyrinth-channel emitter, Biosyst. Eng. 172 (2018) 154–164.
[32] P.T. Wu, D.L. Zhu, J. Wang, Gravity-fed drip irrigation design procedure for a single-manifold subunit, Irrigat. Sci. 28 (2010) 359–369.
[33] L. Zhang, B.Y. Fu, X. Hui, N.W. Ren, Simplified method for estimating throw radius of rotating sprinklers on sloping land, Irrig 36 (2018) 329–337.
[34] H. Li, P. Tang, C. Chen, Z. Zhang, H. Xia, Research status and development trend of fertilization equipment used infertigation in China, Journal of Drainage and Irrigation Machinery Engineering 39 (2) (2021) 200–209.
[35] S. Shin, S. Bae, Simulation of water entry of an elastic wedge using the FDS scheme and HCIB method, J. Hydrodynamics 25 (2013) 450–458.
[36] D. Karmeli, Estimating sprinkler distribution pattern using linear regression, Trans. ASAE (Am. Soc. Agric. Eng.) 21 (1978) 682–686.
[37] J. Liu, X. Zhu, Yuan, S. Li, H.Y. Tang, Research and development trend of agricultural water-saving sprinkler and micro-irrigation equipment in China, Journal of Drainage and Irrigation Machinery Engineering 40 (1) (2022) 87–96.
[38] J.E. Christiansen, Irrigation by Sprinkling. Resolution Bull. 670, Agricultural Experiment Station, University of California, Berkeley, CA, 1942.
[39] R.O. Darko, S.Q. Yuan, J.P. Liu, H.F. Yan, X.Y. Zhu, Overview of advances in improving uniformity and water use efficiency of sprinkler irrigation, Int. J. Agric. Biol. Eng. 10 (2017) 1–15.
[40] Y. Fukui, K. Nakanishi, S. Okamura, Computer elevation of sprinkler uniformity, Irrigat. Sci. 2 (1980) 23–32.